Structure-based 3D-QSAR studies on heteroarylpiperazine derivatives as 5-HT3 receptor antagonists

ARTICLE *in* EUROPEAN JOURNAL OF MEDICINAL CHEMISTRY · AUGUST 2007

Impact Factor: 3.45 · DOI: 10.1016/j.ejmech.2006.12.029 · Source: PubMed

4 AUTHORS, INCLUDING:

Yun Tang
East China University of Science and Techn...
150 PUBLICATIONS **2,169** CITATIONS
SEE PROFILE

De-Yong Ye
Fudan University
44 PUBLICATIONS **130** CITATIONS
SEE PROFILE

Available online at www.sciencedirect.com
ScienceDirect
European Journal of Medicinal Chemistry 42 (2007) 977–984
EUROPEAN JOURNAL OF MEDICINAL CHEMISTRY
http://www.elsevier.com/locate/ejmech

Original article

Structure-based 3D-QSAR studies on heteroarylpiperazine derivatives as 5-HT_3 receptor antagonists

Ya-Ju Zhou [a], Li-Ping Zhu [a], Yun Tang [b,*], De-Yong Ye [a,**]

[a] *Department of Medicinal Chemistry, School of Pharmacy, Fudan University, 138 Yixueyuan Road, Shanghai 200032, China*
[b] *School of Pharmacy, East China University of Science and Technology, 130 Meilong Road, Shanghai 200237, China*

Received 16 June 2006; received in revised form 13 December 2006; accepted 19 December 2006
Available online 13 January 2007

Abstract

Structure-based 3D-QSAR studies were performed on a series of novel heteroarylpiperazine derivatives as 5-HT_3 receptor antagonists with comparative molecular field analysis (CoMFA) and comparative molecular similarity indices analysis (CoMSIA) methods. The compounds were initially docked into the binding pocket of the homology model of 5-HT_3 receptor using GOLD program. The docked conformations with the highest score were then extracted and used to build the 3D-QSAR models, with cross-validated r^2_{cv} values 0.716 and 0.762 for CoMFA and CoMSIA, respectively. The CoMFA and CoMSIA contour plots were also fitted into the 3D structural model of the receptor to identify the key interactions between them, which might be helpful for designing new potent 5-HT_3 receptor antagonists.

Keywords: Structure-based 3D-QSAR; CoMFA; CoMSIA; 5-HT_3 receptor

1. Introduction

5-HT_3 receptor is a prototypical member of the Cys-loop ligand-gated ion channel (LGIC) superfamily, which also includes the glycine (Gly), type A γ-amino butyric acid (GABA$_A$) and nicotinic acetylcholine (nACh) receptors. The ion channel of 5-HT_3 receptor is assembled with five subunits and each subunit is thought to possess an N-terminal ligand binding domain, four transmembrane (TM) domains and a large intracellular loop connecting the third and fourth TM domains [1]. There are two main subtypes of 5-HT_3 receptors: (1) 5-HT_{3A}, a neuronal receptor directly coupled to cation-selective (Na^+, K^+, Ca^{2+}, Mg^{2+}, and other ions) channels, which has structural and functional similarity with the nACh, GABA$_A$, Gly and other ligand-gated ion channels, and (2) 5-HT_{3B}, a regulatory subunit able to modulate the intrinsic channel activity of 5-HT_{3A}. The subunit 5-HT_{3A} is homo-oligomeric while 5-HT_{3B} is heteromeric [2].

Electron microscope images of the purified 5-HT_3 receptor are available in the literature [3] but its three-dimensional (3D) structure has not yet been resolved at atomic level. However, the structure of *Limnaea* acetylcholine binding protein (AChBP) has been determined by X-ray crystallography recently, which is also a member of LGICs, and shares 20% homologous sequence with the extracellular domain of 5-HT_3 receptor [4]. Therefore, a homology model of the extracellular domain of human 5-HT_3 receptor was built based on the crystal structure of AChBP, and some known ligands were docked into the binding site to validate the model [5]. During the process of our work, a similar study using a range of antagonists was published, too [6].

QSAR study has long been used in elucidating mechanism of drug action and optimizing lead compound. When the 3D structure of drug target is also available, structure-based drug design methods can be combined with QSAR method, i.e. structure-based QSAR study, which could provide more information for lead optimization. In this work, a new kind of 5-HT_3

* Corresponding author. Tel.: +86 21 64251052.
** Corresponding author. Tel.: +86 21 54237559; fax: +86 21 64042268.
E-mail addresses: ytang234@ecust.edu.cn (Y. Tang), dyye@shmu.edu.cn (D.-Y. Ye).

0223-5234/$ - see front matter © 2007 Elsevier Masson SAS. All rights reserved.
doi:10.1016/j.ejmech.2006.12.029

antagonists, arylpiperazine derivatives containing quipazine quinoline nucleus with different substituents in 3, 4 and 4′ positions (Scheme 1), were collected from the literature [7]. The compounds were docked into the binding site of the previously reported homology model of the receptor [5] at first, the docking conformations were then performed by 3D-QSAR studies to understand the interaction between the receptor and ligands and to optimize the lead compound with comparative molecular field analysis (CoMFA) [8] and comparative molecular similarity indices analysis (CoMSIA) [9] methods.

2. Materials and methods

2.1. Data set

Totally 35 heteroarylpiperazines were collected from Ref. [7]. They were assayed for their potential ability to displace [^{3}H] granisetron specifically bound to the 5-HT$_3$ receptor in rat cortical membrane [7]. The values of the receptor binding affinities (K_i) were converted to their inverse logarithms. The 35 compounds were randomly divided into training set (28 molecules) and test set (7 molecules) in the ratio of 4:1.

2.2. Molecular modeling

All molecular modeling and statistical analyses were performed on an R14000 SGI Fuel workstation using SYBYL v6.9 molecular modeling software package [10]. The conformation of compound **11**, with the highest affinity value, was constructed using sketch option in SYBYL. Systematic conformation search and energy minimization were performed on the molecule with Gasteiger–Hückel charge and Tripos force field. The other 34 compounds were constructed on the basis of the structure of compound **11**. All molecules were set in their unprotonated state. The 3D structure of extracellular domain of human 5-HT$_3$ receptor was previously built on the base of the crystal structure of AChBP [4,5]. It was reported that the aromatic groups of antagonists were supposed to intercalate between aromatic side-chains of the receptor (Trp178-Tyr229, Tyr138-Tyr148); while the basic centers might interact with Glu231 or Glu124 (ionic interaction), and/or Trp85 (cation–π interaction) of the receptor [6]. Therefore, the binding site of the 5-HT$_3$ receptor was defined as residues within a radius of 16 Å from Cα atom of Trp178 in the binding pocket to ensure that most of the residues critical for ligand binding verified/revealed by previous experimental data were included. All molecules were docked into the binding pocket with program GOLD v2.2 [11–13].

The default settings of GOLD were used, and no flipping was allowed.

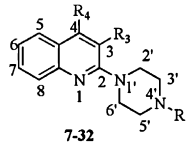

7-32

	R	R_3	R_4
7	CH_3	CH_3	COC_6H_5
8	CH_3	CH_3	$COOCH_2CH_3$
9	CH_3	H	$COOCH_2CH_3$
10	CH_3	CH_2CH_3	$COOCH_2CH_3$
11	CH_3	$CH_2CH_2CH_3$	$COOCH_2CH_3$
12	H	CH_3	$COOCH_2CH_3$
13	CH_3	CH_3	$CON(CH_2)_4$
14	CH_3	CH_3	$CON(CH_2CH_3)_2$
15	CH_3	H	$CON(CH_2CH_3)_2$
16	CH_3	CH_2CH_3	$CON(CH_2CH_3)_2$
17	CH_3	$CH_2CH_2CH_3$	$CON(CH_2CH_3)_2$
18	CH_3	CH_3	$CON(CH(CH_3)CH_3)_2$
19	CH_3	CH_3	$CON(CH_2CH_2CH_3)_2$
20	CH_3	H	$CON(CH_2CH_2CH_3)_2$
21	CH_3	CH_2CH_3	$CON(CH_2CH_2CH_3)_2$
22	CH_3	$CH_2CH_2CH_3$	$CON(CH_2CH_2CH_3)_2$
23	CH_3	CH_3	$CON(CH_2CH_2CH_2CH_3)_2$
24	CH_3	CH_3	$CON(CH_2CH_2CH_2CH_2CH_3)_2$
25	CH_3	CH_3	$CON(CH_2CH_2CH_2CH_2CH_2CH_3)_2$
26	CH_3	CH_3	$CON(CH_3)CH_2C_6H_5$
27	CH_3	H	$CON(CH_3)CH_2C_6H_5$
28	CH_3	CH_2CH_3	$CON(CH_3)CH_2C_6H_5$
29	CH_3	$CH_2CH_3CH_3$	$CON(CH_3)CH_2C_6H_5$
30	CH_3	CH_3	$CON(CH_3)CH_2C{\equiv}CH$
31	CH_3	CH_3	$CON(CH_3)$*p*-Cl-C_6H_4
32	CH_3	CH_2OH	CH_2OH
33	CH_3	$COOC_2H_5$	CH_3

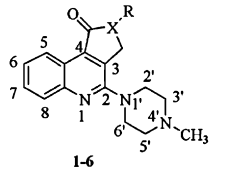

1-6

	X	R
1	N	CH_3
2	N	CH_2CH_3
3	N	$CH_2CH_2CH_3$
4	N	$CH(CH_3)CH_2CH_3$
5	N	$CH_2C_6H_5$
6	O	

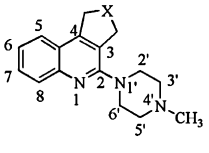

34-35

	X
34	CH_2CH_2
35	CH_2

Scheme 1. Structures and actual pK_i values of molecules used for 3D-QSAR studies [7].

2.3. CoMFA and CoMSIA

The docked conformation with the highest score of each molecule in the training set was superimposed onto a 3D grid box with 2 Å grid. CoMFA fields were formed using sp^3 carbon probe atom carrying +1 charge to generate steric (Lennard–Jones potential) and electrostatic (Coulomb potential) fields at each grid point. The CoMFA fields were scaled by the CoMFA-standard method in SYBYL. A 30 kcal/mol energy cutoff was applied. A distance dependent Gaussian type functional form was employed. The default value of 0.3 was used as the attenuation factor. Similarly, a data table was constructed from similarity indices calculated at the intersections of a regularly spaced lattice (2 Å grid) in CoMSIA.

2.4. PLS analysis and validation of QSAR models

The CoMFA/CoMSIA fields combined with observed biological activities (pK_i) were included in a molecular spreadsheet and the partial least square (PLS) methods were used to generate 3D-QSAR models [14]. To check statistical significance of the models, cross-validations analysis performed by the leave-one-out (LOO) [15] procedure was done to choose optimum number of components (N) [16], subsequently used to derive the final QSAR models. All cross-validated PLS analyses were performed with a column filter value of 2.0. The optimal numbers of components were selected on the basis of the highest cross-validated correlation coefficient (r^2_{cv}), which is defined as follows:

$$r^2_{cv} = 1 - \frac{\sum (Y_{predicted} - Y_{actual})^2}{\sum (Y_{actual} - Y_{mean})^2}$$

where $Y_{predicted}$, Y_{actual}, and Y_{mean} are predicted, actual, and mean values of the target property (pK_i), respectively. The CoMFA/CoMSIA results were graphically interpreted by field contribution maps using the 'STDEV*COEFF' field type.

To assess the predictive power of the 3D-QSAR models derived using training set, biological activities of the test set molecules were predicted. The predictive r^2 (r^2_{pred}) value is calculated as follows:

$$r^2_{pred} = (SD - PRESS)/SD$$

where SD is the sum of squared deviations between the biological activity of the test set and the mean activity of training set molecules, and PRESS is the sum of squared deviations between the actual and the predicted activities of the test set molecules. In addition, the r^2_{cv}, r^2_{pred} and number of components, the conventional correlation coefficient r^2 and its standard error were also computed for each model.

3. Results and discussion

The docked conformations of the molecules in the training set are shown in Fig. 1a. The superposition showed that the ligands fit the binding pocket consisting of critical residues. The

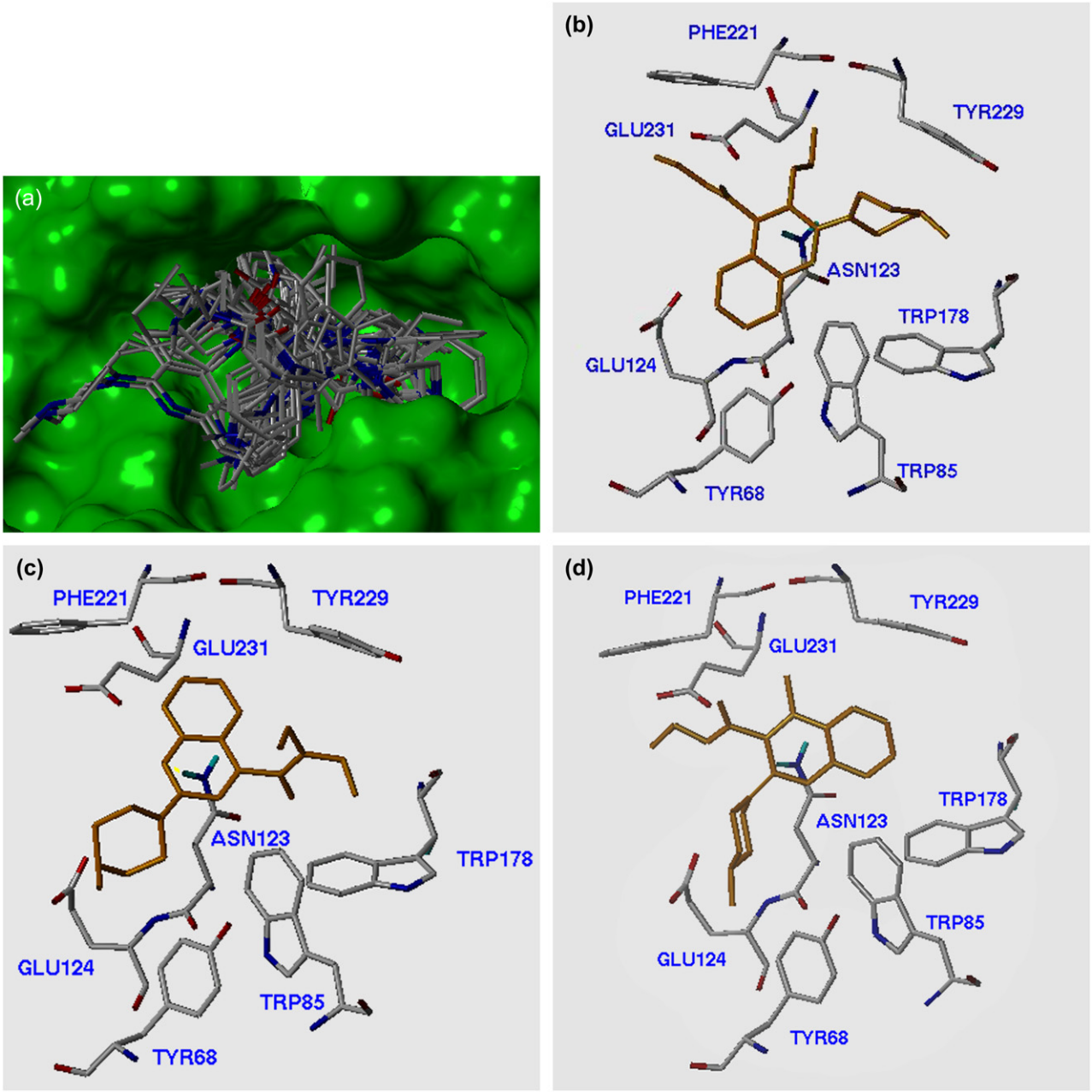

Fig. 1. (a) The docked conformations of the molecules in the training set together with the binding site of 5-HT_3 receptor. The solvent-accessible surface is indicated as a solid surface. (All hydrogen atoms were omitted.) (b) The docked conformations of molecules whose piperazine ring located between Trp85 and Tyr229 of the receptor and compound **11** was showed as a representative. (c) The docked conformations of molecules whose C-4 substituent located between Trp85 and Tyr229 of the receptor and the representative was compound **15** whose nitrogen atom in the quinoline ring formed hydrogen bond with Asn123 of the receptor. (d) The docked conformations of compound **33** whose phenyl ring was located between Trp85 and Tyr229 of the receptor (the hydrogen bonds are shown in yellow lines).

piperazine ring of most ligands located between Trp85 and Tyr229 of the receptor (Fig. 1b) among which compounds **29** and **30** formed hydrogen bonds with Asn123 of the receptor. However, some other ligands seemed to have their C-4 substituent located between Trp85 and Tyr229 of the receptor (Fig. 1c). And most of their nitrogen atom in the quinoline ring (i.e. **15**, **16**, etc.) formed hydrogen bond with Asn123 of the receptor, while in compounds **24** and **25** the hydrogen bonds were formed by the carbonyl group of their C-4 substituents. Compounds **33** and **35** whose phenyl ring located between Trp85 and Tyr229 of the receptor had different conformations with others (Fig. 1d). These observations seem to be different from the pharmacophore models mentioned above [6]. Therefore, they might reveal a novel interaction mode between 5-HT_3 receptor and antagonists. And the results of the docking studies and 3D-QSAR would offer constructive suggestions to the further rectification of the receptor model. And it might be helpful for designing new potent 5-HT_3 receptor antagonists.

Considering the ionization of the compounds in physiological pH, we also did the 3D-QSAR studies on the protonated molecules, but worse results were obtained. Therefore, unprotonated state of each molecule was used in the study.

3.1. CoMFA

The statistical details of CoMFA are summarized in Table 1. The cross-validated value, r^2_{cv}, was 0.716, with an optimum number of six components. This analysis was used for final non-cross-validated run, giving a correlation coefficient of 0.992 showing a good linear correlation between the observed and predicted activities of the molecules in the training set. These statistical indexes were reasonably high, indicating that the CoMFA model might have a credible predictive ability. The experimental pK_i, predictive pK_i and residual values by CoMFA and CoMSIA are given in Table 2. The introduction of lipophilicity log P values (calculated with XLOGP 2.0. [17]) did not improve the CoMFA models.

Table 1
Summary of results from the CoMFA and CoMSIA analysis

	r^2_{cv} [a]	N[b]	r^2[c]	SEE[d]	F[e]
CoMFA	0.716	6	0.992	0.073	433.222
CoMSIA (S + E)	0.789	6	0.979	0.118	162.425
CoMSIA (S + E + H)	0.783	6	0.984	0.104	213.510
CoMSIA (S + E + A)	0.735	6	0.972	0.138	119.469
CoMSIA (S + E + D)	0.789	6	0.979	0.118	162.425
CoMSIA (S + E + H + D)	0.783	6	0.984	0.104	213.510
CoMSIA (S + E + H + A)	0.762	6	0.982	0.109	191.578
CoMSIA (S + E + D + A)	0.735	6	0.972	0.138	119.469
CoMSIA (S + E + H + D + A)[f]	0.762	6	0.982	0.109	191.578

[a] Leave-one-out (LOO) cross-validation correlation coefficient.
[b] Optimum number of components.
[c] Non-cross-validation correlation coefficient.
[d] Standard error of estimate.
[e] F-test value.
[f] S, E, H, D, and A represent the steric, electrostatic, hydrophobic, hydrogen bond donor and acceptor property fields, respectively.

Table 2
Experimental pKi, predictive pKi and residual values by CoMFA and CoMSIA

Compound	Actual pKi	Predicted pKi		Residual values	
		CoMFA	CoMSIA	CoMFA	CoMSIA
Training set					
1	8.68	8.667	8.727	0.013	−0.047
2	8.52	8.538	8.542	−0.018	−0.022
3	8.44	8.408	8.423	0.032	0.017
4	8.38	8.381	8.330	−0.001	0.005
5	8.21	8.215	8.233	−0.050	−0.023
7	9.08	9.029	8.931	0.051	0.149
8	9.37	9.410	9.411	−0.040	−0.041
9	9.07	9.112	9.078	−0.042	−0.008
10	9.68	9.730	9.720	−0.050	−0.040
11	10.10	10.103	10.127	−0.003	−0.027
14	9.43	9.368	9.351	0.062	0.079
15	8.80	8.875	8.937	−0.075	−0.137
16	9.29	9.248	9.222	0.042	0.068
17	9.04	9.043	9.140	−0.003	−0.100
18	8.66	8.705	8.693	−0.045	−0.033
20	9.17	9.083	9.083	0.087	0.087
21	8.96	8.944	8.943	0.016	0.017
22	8.92	8.984	8.892	−0.064	0.028
23	9.11	9.133	9.209	−0.023	−0.099
24	7.72	7.640	7.435	0.080	0.285
25	6.73	6.891	6.949	−0.161	−0.219
26	9.26	9.336	9.268	−0.076	−0.008
27	9.39	9.313	9.287	0.077	0.103
28	8.00	7.911	7.976	0.089	0.024
29	7.85	7.787	7.932	0.063	−0.082
30	9.35	9.259	9.289	0.091	0.061
33	9.77	9.866	9.841	−0.096	−0.071
35	9.62	9.592	9.603	0.028	0.017
Test set					
6	8.62	8.574	8.783	0.046	−0.163
12	9.25	9.270	9.312	−0.020	−0.062
13	8.80	8.970	9.036	−0.170	−0.236
19	9.96	9.342	9.357	0.618	0.603
31	7.89	7.968	7.998	−0.078	−0.108
32	8.57	8.842	8.558	−0.272	0.012
34	9.64	9.360	9.342	0.280	0.298

The electrostatic field descriptor explained 63.4% of the variance while the proportion of steric descriptor accounted for 36.6%. Therefore, the electrostatic field had greater influence than the steric field. These electrostatic and steric fields are presented as contour plots in Fig. 2a and b, respectively.

3.2. CoMSIA

The CoMSIA results are also summarized in Table 1. A cross-validated value, r^2_{cv} of 0.762 and a non-cross-validation correlation coefficient r^2 of 0.982 were obtained. The F value and standard error are 191.578 and 0.109, respectively. These data also indicated that a reliable CoMSIA model was successfully constructed. The hydrogen bond acceptor (A) field descriptor explained 24.9% of the variance and the steric (S) descriptor only contributed 11.7%, while the proportion of electrostatic (E) and hydrophobic (H) descriptor accounted for 32.4% and 31.0%, respectively. The hydrogen bond donor field was ignored for all the compounds in the training set

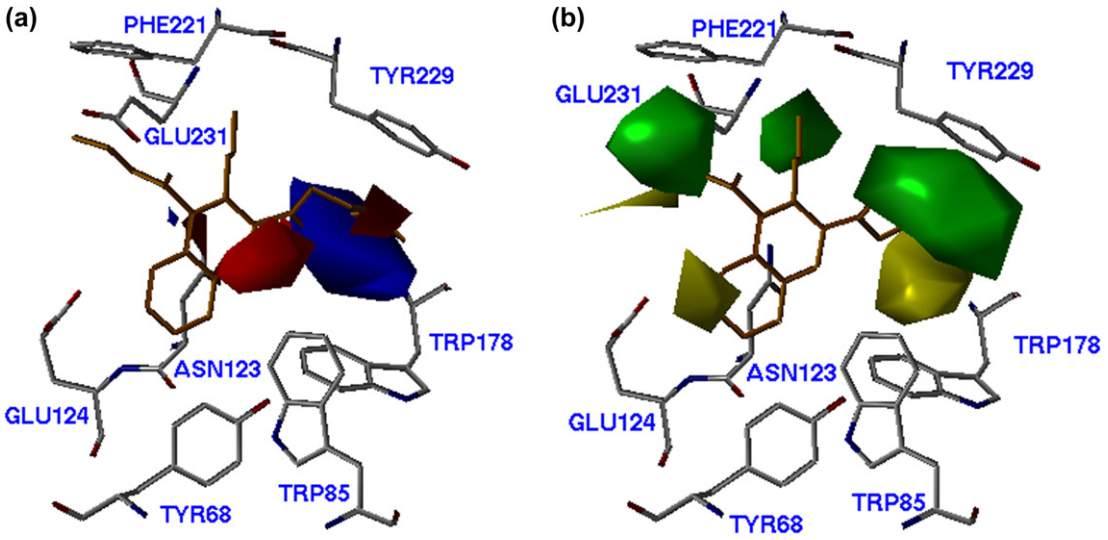

Fig. 2. Mapping the CoMFA contours in the active site of 5-HT_{3A} receptor with compound **11** as an example. The ligand was shown in orange. The contour plots (STDEV*COEFF) of the CoMFA: (a) electrostatic fields; blue contours indicated regions where electropositive groups increase activity, whereas red contours indicated regions where electronegative groups increase activity and (b) steric fields; green contours indicated regions where bulky groups increase activity, whereas yellow contours indicated regions where bulky groups decrease activity (all hydrogen atoms of the receptor were omitted).

which did not have any hydrogen bond donor. Therefore, the electrostatic, hydrophobic and acceptor fields had greater effluence than steric. All the fields are also shown as contour plots in Fig. 3a–d, respectively. The addition of lipophilicity log *P* (calculated as mentioned above) to the set of independent variable did not improve the correlation either.

3.3. Validation of 3D-QSAR models

The test set was applied to evaluate the predictive power of the CoMFA and CoMSIA 3D-QSAR models. Fig. 4 shows the plots of actual versus predicted activity for both training set and test set. In almost all cases of 3D-QSAR models, the predicted values fell close to the observed pK_i values, deviating by not more than 0.7 logarithmic units. Finally, CoMFA and CoMSIA showed similar predictive power with respect to these seven compounds (r^2 values for CoMFA and CoMSIA are 0.808 and 0.816, respectively).

3.4. Structure-based analysis of receptor–ligand interactions

The data in Table 1 show that the CoMFA electrostatic field descriptor explained 63.4% of the variance, while the steric descriptor explained the rest 36.6%. These electrostatic and steric fields are presented as contour plots in Fig. 2a and b, respectively.

As shown in Fig. 2a, there was a major blue region near the C-5′ position of the quipazine quinoline nucleus, one of which was also located near Trp178, indicating that substitution of electropositive group at this position would increase the activity. (For interpretation of the references to colour in text the reader is referred to the web version of this article.) There are two red contours: one was near the N-1 atom and the other was close to N-1′of the quipazine quinoline nucleus corresponding to Trp85 of the receptor. Presence of red contours emphasized that electronegative group was desirable at this position. The carbonyl group of compound **33** was around the red region which could explain better activity. And compound **24** exhibited low activity as its carbonyl group was close to the blue region and its alkyl substituent in C-3 position was near to the red region.

The steric contour map (Fig. 2b) showed a major yellow region near the N-4′ position of the quipazine quinoline nucleus corresponding to the Trp178 of the 5-HT_3 receptor, indicated that any bulky substituent decreased activity. The methyl on the terminal piperazine nitrogen appeared in the bigger yellow region resulting in that compound **28** had weak activity. However, there were one major green region surrounding piperazine and two green regions nearing the C-3 and C-4 positions of the quipazine quinoline nucleus, respectively (Scheme 1), indicating that a bulky substituent was preferred to produce higher activity. The conformation of the substituent in C-4 position may affect the activity. Compound **10** whose ethyl in C-3 position was close to the green region showed higher activity than compound **8**. Compound **11** had the best activity as the conformation occupies most of the green regions.

Fig. 3 depicts the CoMSIA coefficient contour maps with compound **11** displayed for visualization. As shown in Fig. 3a, the electrostatic fields were represented by white- and yellow-colored contours (white, positive charge favored; yellow, electronegative group favored). There was a major white regions in the contour map located near C-5′ position of the quipazine quinoline nucleus, between Trp178 and Tyr229 of the receptor. Compound **26** which oriented its carbonyl group into the yellow region located near the terminal piperazine nitrogen and located its nitrogen in N-1′ position

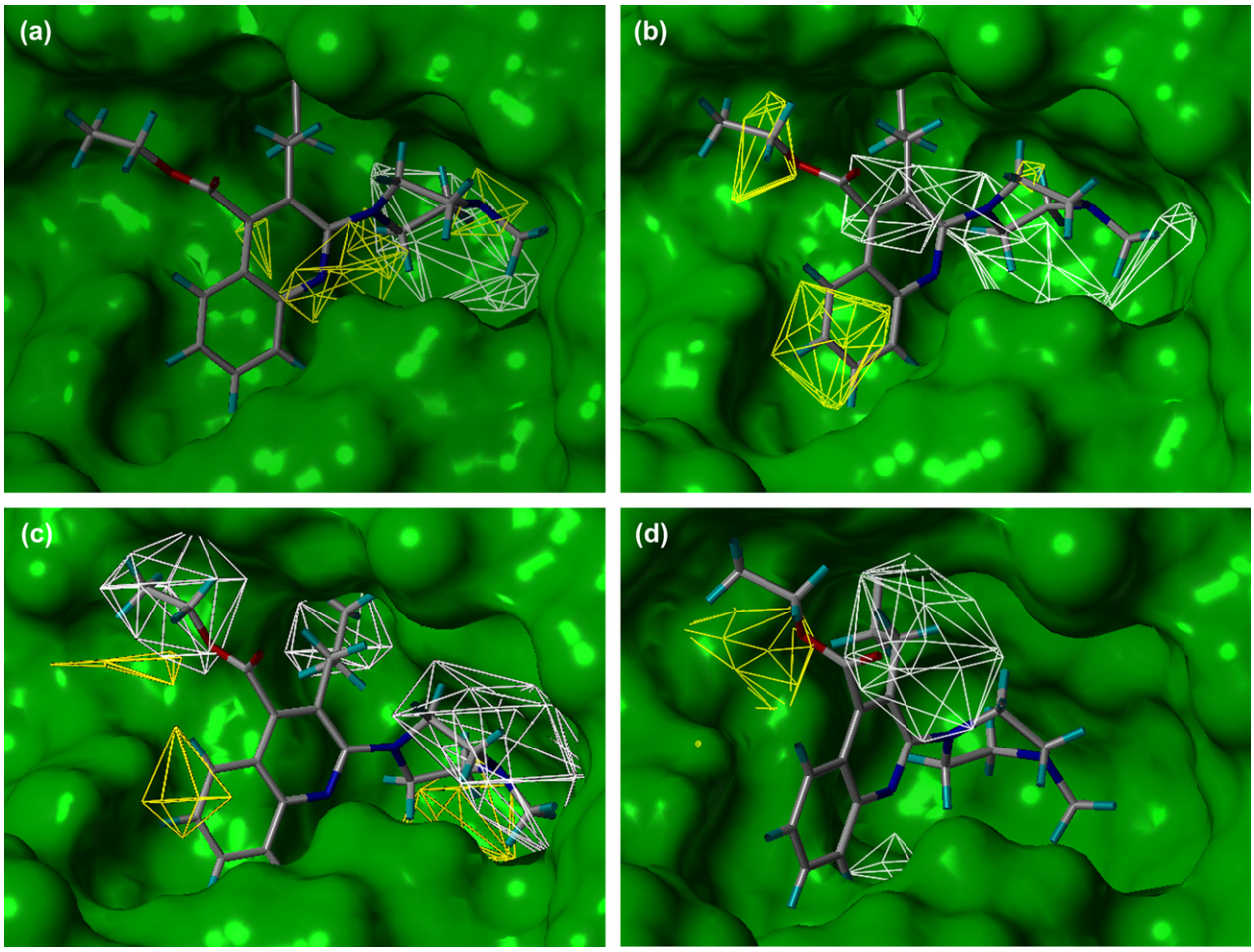

Fig. 3. Contour plot of the CoMSIA STDEV*COEFF for (a) electrostatic properties: White isopleths encompass regions where an increase of positive charge would enhance affinity, whereas in yellow contoured areas more negative charges were favorable for binding properties. (b) Hydrophobic properties: White isopleths encompass regions favorable for hydrophobic groups, whereas in yellow contoured areas more hydrophilic groups were favorable for binding properties. The solvent-accessible surface was indicated as a solid surface. (c) Steric features: White isopleths enclose areas where steric bulk would enhance affinity. Yellow contours highlight areas which should be kept unoccupied. (d) Acceptor fields (white, favored; yellow, disfavored).

near the bigger yellow region around the N-1 position of the quipazine quinoline showed better binding affinity than compound **5**. In the mean time, it was to be explained that compound **21** had worse activity for its two nitrogen atom in piperazine which was occupied by the white region when compared to compound **10**. The distribution of electrostatic contours in this model was almost consistent with that of CoMFA (Fig. 2a).

The hydrophobic contours are shown in Fig. 3b. The white hydrophobic contours indicate that hydrophobic substituents would be good for increasing the potency, while hydrophilic substituents are beneficial to the activity at the regions of yellow contours. There was a large white area near N-1, C-5′ and C-6′ positions of the quipazine quinoline nucleus indicating that any lipophilic group was preferred at this position. Compounds **24** and **25** oriented their nitrogen atoms in C-4 position of quipazine quinoline nucleus into the white contoured region resulting in low activity. Compound **5** showed lower activities than compound **2** for its bigger phenyl substitute occupied the yellow contoured region, which was occupying the C-6 position of the quipazine quinoline nucleus. As for the receptor, the white region should correspond to the hydrophobic residues whereas the yellow ones should be close to the polar residues. Actually, the yellow regions one of which was near Trp68 and the other around Phe221. Therefore, the position of Trp68 and Phe221 might be rectified.

The steric field contour plots are displayed in Fig. 3c. It was indicated that a large group in white regions would be beneficial to the binding affinity. Three major white regions were found: one was located between the Trp85 and Tyr229 of the receptor, occupying the C-3′ position of the quipazine quinoline nucleus, and the other two were around the C-3 and C-4 positions of the quipazine quinoline nucleus between the Phe221 and Glu231 of the receptor. This could explain why compound **29** showed lower affinity than compound **27** whose phenyl ring in the C-4 substitution came into the white region. It was observed that bulky substituent in yellow regions, which was located near C-5 and C-6 positions of the quipazine quinoline nucleus and 3′, 4′, 5′ positions of the piperazine ring, respectively, would decrease the affinity. The result was in accordance with the contours of the CoMSIA hydrophobic field. Therefore, compound **5** whose phenyl

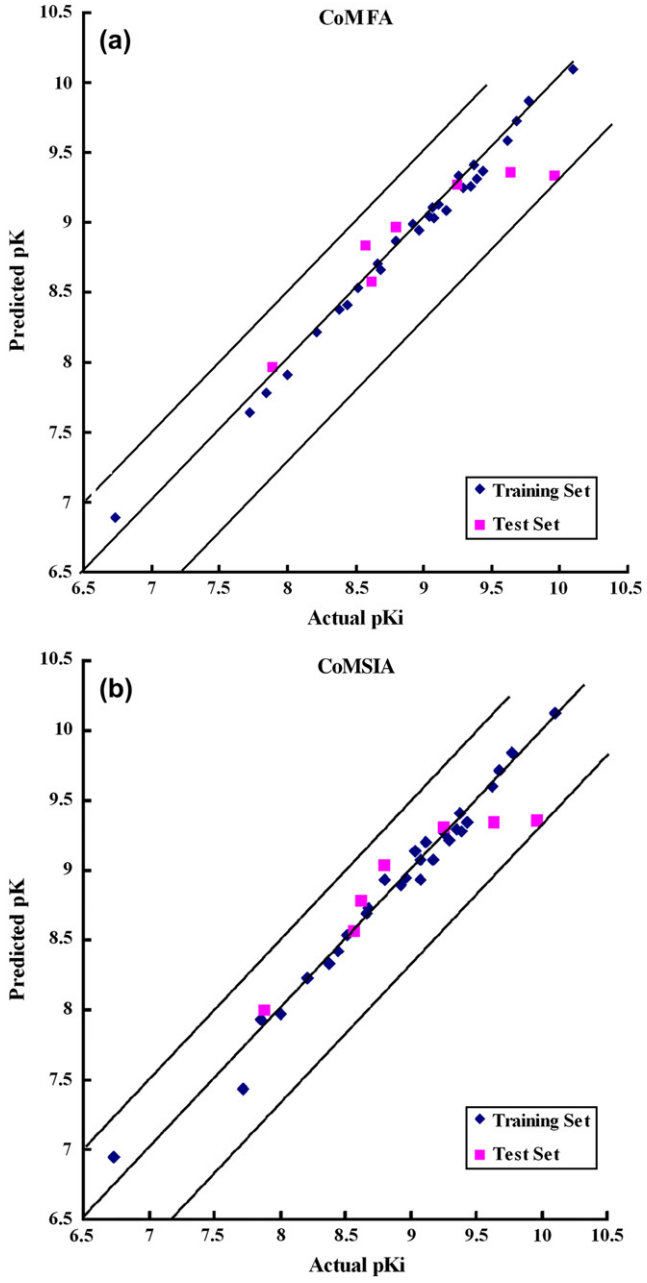

Fig. 4. Actual versus predicted pK_i of training and test set molecules for (a) CoMFA and (b) CoMSIA 3D-QSAR models.

group of the pyrrolidone ring entered the yellow region had lower activity than compound **4**.

The hydrogen bond acceptor contours are displayed in Fig. 3d. The existence of one white region near carbonyl group implied that there might exist hydrogen bond donor at the corresponding positions of the receptor's active site (Trp85, Tyr148 and Tyr229), consisted with our homology model. This observation clearly indicated that hydrogen bond acceptor near the white contours would increase the activity. A yellow contour near C-3 position of the quipazine quinoline nucleus indicated that molecules with hydrogen bond acceptor at this position would be less active. Therefore, compound **22** whose carbonyl group closer to the white region revealed higher affinities than compound **29** whose carbonyl group occupied the yellow region.

The results showed that a moderately bulky substituent at the C-4 position was preferred to produce higher binding affinities. Introduction of some proper alkyl substituents to the C-5′ and C-6′ positions of piperazine may improve the binding affinities. The bicyclic derivatives showed better affinity than the corresponding tricyclic ones (i.e. compare compound **8** with **2**). The set of compounds was worthy of further studies.

4. Summary

In this study, CoMFA and CoMSIA 3D-QSAR analyses were performed on the docked conformations of 28 heteroarylpiperazines as 5-HT_3 receptor antagonists. Both models showed good prediction capabilities in terms of r^2_{cv} and r^2 values, while CoMFA model showed better predictive ability [SEE (standard error of estimate) = 0.073)] than CoMSIA one (SEE = 0.109). The good correlation between experimental and predicted bioactivities for seven compounds in test set further verified the reliability of the constructed QSAR models. The CoMFA model provided the most significant correlation of steric and electrostatic fields with the biological activities. The effects of the electrostatic, hydrophobic, steric and hydrogen bond acceptor fields around the aligned molecules on their activities were clarified by analyzing the CoMSIA contour maps. The original intention of designing the heteroarylpiperazines was to analyze the activity influence of compounds with different hydrophobic group [7]. In this study, we found some implications could be drawn to improve the activity and selectivity of heteroarylpiperazines as 5-HT_3 receptor antagonists. For example, moderately bulky hydrophobic electropositive group substituent at the C-4 position and the introduction of some proper alkyl substituents to the C-5′ and C-6′ positions of piperazine might be preferable to produce higher activity. Therefore, the results would be very helpful for further structural modification of heteroparylpiperazines.

Acknowledgments

We are grateful to Dr. Wei Li for his support and encouragement.

References

[1] G.F. Lopreato, P. Banerjee, Mol. Brain Res. 118 (2003) 45–51.
[2] Z.H. Israili, Curr. Med. Chem. – Central Nervous System Agents 1 (2001) 171–199.
[3] F.G. Boess, I.L. Martin, Neuropharmacology 33 (1994) 275–317.
[4] K. Brejc, W.J. Van Dijk, R.V. Klaassen, M. Schuurmans, J. Van der Oost, A.B. Smit, T.K. Sixma, Nature (2001) 269–411.
[5] L.-P. Zhu, D.-Y. Ye, Y. Tang, J. Mol. Model. 13 (2007) 121–131.
[6] G. Maksay, Z. Bikádi, M.J. Simonyi, J. Recept. Signal Transduct. Res. 23 (2003) 255–270.
[7] A. Cappelli, A. Gallelli, J. Med. Chem. 48 (2005) 3564–3575.
[8] R.D. Cramer III, D.E. Patterson, J.D. Bunce, J. Am. Chem. Soc. 110 (1998) 5959–5967.

[9] G. Klebe, U. Abraham, T.J. Mietzner, J. Med. Chem. 37 (1994) 4130–4146.
[10] SYBYL v6.9 Molecular Modeling Software, Tripos Associates, Inc.: 1669, South Hanley Road, Suite 303, St. Louis, Missouri, MO 63144-2913, USA. <http://www.tripos.com>.
[11] GOLD v2.2 CCDC Software Ltd., 12 Union Road, Cambridge CB2 1EZ, United Kingdom. http://www.ccdc.cam.ac.uk.
[12] G. Jones, P. Willett, R.C. Glen, A.R. Leach, R. Taylor, J. Mol. Biol. 267 (1997) 727–748.
[13] G. Jones, P. Willett, R.C. Glen, J. Mol. Biol. 245 (1995) 43–53.
[14] S. Wold, A. Ruhe, H. Wold, W.J. Dunn III, SIAM J. Sci. Stat. Comput. 5 (1984) 735–743.
[15] R.D. Cramer III, J.D. Bunce, D.E. Patterson, Quant. Struct.–Act. Relat. 7 (1988) 18–25.
[16] B.L. Bush, R.B. Nachbar Jr., J. Comput. Aided Mol. Des 7 (1993) 587–619.
[17] R. Wang, Y. Fu, L. Lai, J. Chem. Inf. Comput. Sci. 37 (1997) 615–621.<http://mdl.ipc.pku.edu.cn/>.